Catalysis-Induced Phase Separation and Autoregulation of Enzymatic Activity

Matthew W. Cotton,[1,2] Ramin Golestanian,[2,3,*] and Jaime Agudo-Canalejo[2,†]
[1]Mathematical Institute, University of Oxford, Woodstock Road, Oxford, OX2 6GG United Kingdom
[2]Department of Living Matter Physics, Max Planck Institute for Dynamics and Self-Organization, D-37077 Göttingen, Germany
[3]Rudolf Peierls Centre for Theoretical Physics, University of Oxford, Oxford OX1 3PU, United Kingdom

(Received 27 May 2022; accepted 9 September 2022; published 3 October 2022)

We present a thermodynamically consistent model describing the dynamics of a multicomponent mixture where one enzyme component catalyzes a reaction between other components. We find that the catalytic activity alone can induce phase separation for sufficiently active systems and large enzymes, without any equilibrium interactions between components. In the limit of fast reaction rates, binodal lines can be calculated using a mapping to an effective free energy. We also explain how this catalysis-induced phase separation can act to autoregulate the enzymatic activity, which points at the biological relevance of this phenomenon.

DOI: 10.1103/PhysRevLett.129.158101

Introduction.—Liquid-liquid phase separation has emerged in recent years as a key principle governing intracellular organization [1,2]. It is generally believed that the main drivers of phase separation in such systems are the attractive equilibrium interactions between the different soluble components, which are needed to overcome the entropic costs associated with phase separation [3,4]. The emergence of condensates that are enriched or depleted in specific molecules can be designed by tuning these interactions [5–8]. On the other hand, it is clear that intracellular environments are far from being at thermodynamic equilibrium, and that the possible effects of nonequilibrium activity on phase separation need to be taken into consideration [9–15]. In all of these studies, however, equilibrium interactions have remained the driving force for phase separation; nonequilibrium effects have entered only as additional chemical reactions that convert the phase-separating components into each other [9–11] or, in a coarse-grained description, as gradient [11–13] or nonreciprocal [14,15] terms that do not derive from a free energy. These nonequilibrium effects, albeit not driving the phase separation process, may for example affect the size distribution and coarsening dynamics of the resulting condensates, or lead to the formation of static and moving micropatterns.

Biomolecular condensates are often rich in enzymes that catalyze chemical reactions, in which case they are known as metabolons [16]. Such enzyme-rich condensates can also be assembled *in vitro* [17]. The packing of enzymes in close proximity to each other can cause changes in metabolic and enzymatic rates when compared to a homogeneous system, for example by substrate channeling, where an intermediate product in a cascade reaction is passed on between enzymes [18], or by mechanical effects that alter the catalytic rate [19]. Moreover, it has been suggested that biological systems can self-organize the cell cycle dynamics to lower the overall rate of metabolic activity and the ensuing free energy dissipation [20]. While the mechanisms underlying both the formation of enzyme-rich condensates and metabolic autoregulation are currently not well understood [16,20], it would be interesting to investigate whether such behaviors can generically emerge from spatial organization that arises from catalysis-induced nonequilibrium activity.

Here, we propose a fundamentally new mechanism for the formation of enzyme-rich condensates, which does not rely on equilibrium attractive interactions between enzymes, but rather on effective interactions that arise purely as a consequence of their nonequilibrium catalytic activity (see Fig. 1 for a schematic of the phenomenon and Fig. 2 for the corresponding phase diagrams). While effective interactions mediated by self-generated chemical gradients have been previously described in the context of phoretic active colloids or chemotactic microorganisms [21–25], these were based on a microscopic and hydrodynamic description of individual colloid-colloid interactions. The theoretical framework presented here takes a complementary approach based on nonequilibrium thermodynamics and Flory-Huggins theory of suspensions, to manifestly connect the phenomenology to the existing studies on intracellular phase separation [3–10]. We find that this catalysis-induced phase separation (CIPS) can be described by a mapping to an effective free energy, and thus shows equilibrium features

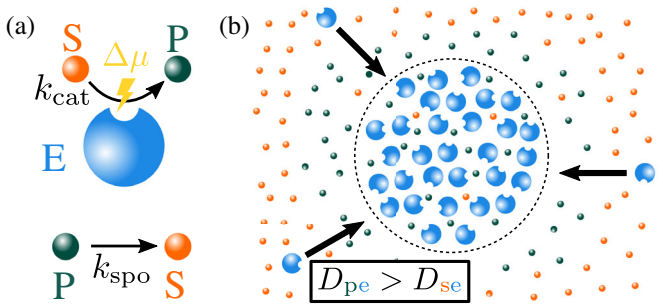

FIG. 1. Processes leading to CIPS. (a) Enzymes convert substrate into product by a fueled catalytic reaction, while product turns into substrate spontaneously. (b) The catalyzed reaction creates gradients of substrate and product around enzyme-rich regions, which attract more enzymes when the off diagonal transport coefficients coupling enzyme fluxes to product and substrate thermodynamic forces satisfy $D_{\mathrm{pe}} > D_{\mathrm{se}}$.

such as the existence of binodal and spinodal lines which meet at a critical point. Moreover, we show that phase separation in this model, which is itself induced by catalysis, generically leads to a decrease in the overall catalytic activity of the system, thus providing a mechanism for the autoregulation of catalytic activity.

Model.—We consider an incompressible fluid with N components described by the volume fractions $\phi_i(\boldsymbol{r}, t)$, each corresponding to individual molecules of volume v_i on the microscopic scale. The Flory-Huggins theory of suspensions gives the free energy of the system as $F = \int d\boldsymbol{r}\, f_{\mathrm{FH}}$, with the free energy density $f_{\mathrm{FH}}(\{\phi_i\}) = \sum_{i=1}^{N}(1/v_i)[\varepsilon_i\phi_i + k_BT\phi_i(\log\phi_i - 1)]$, where ε_i is the enthalpy of component i. Importantly, we do not include any interaction terms in the free energy; in particular, f_{FH} does not contain terms of the usual form $\chi_{ij}\phi_i\phi_j$. This implies that phase separation in this system would be impossible at equilibrium. We denote $\beta \equiv (k_BT)^{-1}$. Each ϕ_i is governed by conserved dynamics $\dot{\phi}_i + \boldsymbol{\nabla}\cdot\boldsymbol{J}_i = 0$ driven by thermodynamic fluxes $\boldsymbol{J}_i = -\sum_{j=1}^{N} M_{ij}\boldsymbol{\nabla}\mu_j$, where $\mu_j = v_j(\delta F/\delta\phi_j) = \varepsilon_j + k_BT\log\phi_j$ is the chemical potential of component j, and M_{ij} is a mobility matrix [26]. Incompressibility of the suspension requires $\sum_{i=1}^{N}\phi_i = 1$, which implies (via the dynamical equations) that the mobilities must satisfy $\sum_i M_{ij} = 0$ [27]. The Onsager reciprocal relations further constrain the form of the mobilities, namely $v_jM_{ij} = v_iM_{ji}$ [26]. These constraints mean that a system of N components has $N(N-1)/2$ free mobilities. In the following, we assume the common form of $M_{ij} = -\beta D_{ij}\phi_i\phi_j$ for $i \neq j$, where the constraints just described imply $M_{jj} = -\sum_{i\neq j} M_{ij}$ and $v_jD_{ij} = v_iD_{ji}$ [6,27–29]. We note that the transport coefficients D_{ij} determine the rate at which the components respond to local effective concentration gradients and exchange positions, and as such are inherently related to the phenomena of diffusiophoresis, cross diffusion, and Maxwell-Stefan diffusion [30].

We make the model active by allowing nonequilibrium (fueled) conversion between two components, substrate (S) and product (P), catalyzed by an enzyme (E). This can be described by the reaction $E + S + F \rightleftharpoons E + P + W$, where F and W represent fuel and waste molecules, respectively. We do not model the dynamics of the fuel and waste here, but assume that the system is in contact with a reservoir that maintains constant chemical potentials, μ_{f} and μ_{w}, and define $\Delta\mu \equiv \mu_{\mathrm{f}} - \mu_{\mathrm{w}}$. Alternatively, $\Delta\mu$ could represent the energy transferred by a photon in a light-activated catalytic reaction. We further allow for spontaneous conversion between S and P, corresponding to the reaction $S \rightleftharpoons P$. Note that incompressibility implies $v_{\mathrm{p}} = v_{\mathrm{s}}$. Using the definition $\Delta\varepsilon \equiv \varepsilon_{\mathrm{s}} - \varepsilon_{\mathrm{p}}$, we can write the net rate of the spontaneous reaction as

$$r_{\mathrm{spo}} = r_{\mathrm{spo}}^{S\to P} - r_{\mathrm{spo}}^{P\to S} = k_{\mathrm{spo}}[e^{\beta\Delta\varepsilon}\phi_{\mathrm{s}} - \phi_{\mathrm{p}}], \tag{1}$$

which entails detailed balance with $r_{\mathrm{spo}}^{S\to P}/r_{\mathrm{spo}}^{P\to S} = \exp[\beta(\mu_{\mathrm{s}} - \mu_{\mathrm{p}})]$. The catalyzed reaction rate will have a similar functional form with an additional dependence on ϕ_{e}, namely

$$r_{\mathrm{cat}} = r_{\mathrm{cat}}^{S\to P} - r_{\mathrm{cat}}^{P\to S} = k_{\mathrm{cat}}\phi_{\mathrm{e}}[\phi_{\mathrm{s}} - \phi_{\mathrm{p}}e^{-\beta(\Delta\varepsilon+\Delta\mu)}], \tag{2}$$

which also entails detailed balance with $r_{\mathrm{cat}}^{S\to P}/r_{\mathrm{cat}}^{P\to S} = \exp[\beta(\mu_{\mathrm{s}} - \mu_{\mathrm{p}} + \Delta\mu)]$. We will typically take $\Delta\varepsilon < 0$ and $\Delta\varepsilon + \Delta\mu > 0$, so that the spontaneous and catalyzed reactions run preferentially in the $P \to S$ and $S \to P$ directions, respectively; see Fig. 1. Combining the conserved dynamics with the reaction terms and defining $R \equiv r_{\mathrm{spo}} + r_{\mathrm{cat}}$ results in the evolution equations for the three-component system

$$\dot{\phi}_{\mathrm{e}} = \boldsymbol{\nabla}\cdot(M_{\mathrm{ee}}\boldsymbol{\nabla}\mu_{\mathrm{e}} + M_{\mathrm{es}}\boldsymbol{\nabla}\mu_{\mathrm{s}} + M_{\mathrm{ep}}\boldsymbol{\nabla}\mu_{\mathrm{p}}), \tag{3}$$

$$\dot{\phi}_{\mathrm{s}} = \boldsymbol{\nabla}\cdot(M_{\mathrm{se}}\boldsymbol{\nabla}\mu_{\mathrm{e}} + M_{\mathrm{ss}}\boldsymbol{\nabla}\mu_{s} + M_{\mathrm{sp}}\boldsymbol{\nabla}\mu_{\mathrm{p}}) - R, \tag{4}$$

$$\dot{\phi}_{\mathrm{p}} = \boldsymbol{\nabla}\cdot(M_{\mathrm{pe}}\boldsymbol{\nabla}\mu_{\mathrm{e}} + M_{\mathrm{ps}}\boldsymbol{\nabla}\mu_{\mathrm{s}} + M_{\mathrm{pp}}\boldsymbol{\nabla}\mu_{\mathrm{p}}) + R. \tag{5}$$

Steady state and stability.—The minimal model [Eqs. (3)–(5)] has a homogeneous steady-state solution when $R = 0$, which is given by any ϕ_{e}^* as well as

$$\phi_{\mathrm{s}}^* = \phi_{\mathrm{s+p}}^* \frac{k_{\mathrm{spo}} + k_{\mathrm{cat}}\phi_{\mathrm{e}}^* e^{-\beta(\Delta\varepsilon+\Delta\mu)}}{k_{\mathrm{spo}} + k_{\mathrm{cat}}\phi_{\mathrm{e}}^* e^{-\beta(\Delta\varepsilon+\Delta\mu)} + k_{\mathrm{spo}}e^{\beta\Delta\varepsilon} + k_{\mathrm{cat}}\phi_{\mathrm{e}}^*} \tag{6}$$

with $\phi_{\mathrm{s+p}}^* = 1 - \phi_{\mathrm{e}}^*$ and $\phi_{\mathrm{p}}^* = \phi_{\mathrm{s+p}}^* - \phi_{\mathrm{s}}^*$.

We can study the linear stability of this homogeneous steady state by considering a small perturbation $\phi_i(\boldsymbol{r}, t) = \phi_i^* + \delta\phi_i(\boldsymbol{r}, t)$. We find that the steady state undergoes an instability at the longest wavelengths provided the following condition holds

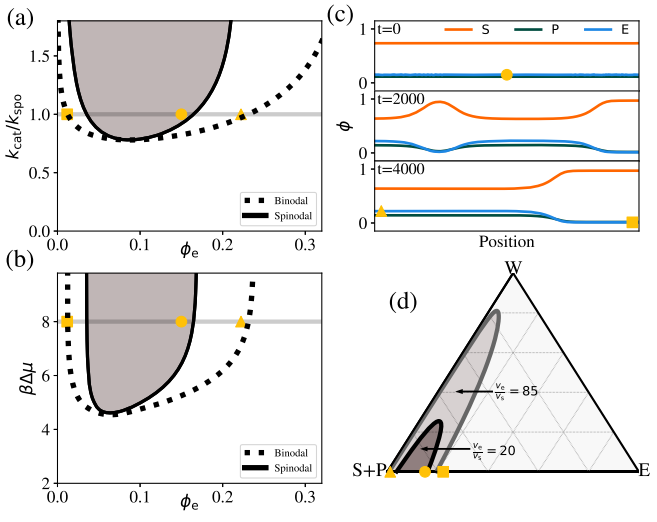

FIG. 2. Phase behavior and onset of CIPS. (a),(b) Spinodal lines [from Eq. (7)] and binodal lines (from the common tangent construction of f_{eff}) for (a) varying k_{cat} with $\Delta\mu = 8k_BT$ and (b) varying $\Delta\mu$ with $k_{\mathrm{cat}}/k_{\mathrm{spo}} = 1$. (c) Numerical simulations showing the evolution of a uniform steady state with $\phi_{\mathrm{e}} = 0.15$ into two phase-separated regions. The circle, triangle, and square identify the homogeneous steady state and the dense and dilute enzyme phases, respectively, and are plotted in all other panels for comparison. (d) Stability diagram of a mixture including a water component, for $\Delta\mu = 8k_BT$ and $k_{\mathrm{cat}}/k_{\mathrm{spo}} = 1$. The darker and lighter shaded regions mark the spinodal regions for $v_{\mathrm{e}}/v_{\mathrm{s}} = 20$ [also used in (a)–(c)] and $v_{\mathrm{e}}/v_{\mathrm{s}} = 85$, respectively. Additional system parameters in (a)–(d) are $\Delta\varepsilon = -5k_BT$, $D_{\mathrm{pe}} = 4D_{\mathrm{se}}$, and $D_{\mathrm{ps}} = 10D_{\mathrm{se}}$; in (d) $D_{\mathrm{ew}} = D_{\mathrm{sw}} = D_{\mathrm{pw}} = 10D_{\mathrm{se}}$ and $v_{\mathrm{w}} = v_{\mathrm{s}}$.

$$\frac{1}{v_{\mathrm{e}}\phi_{\mathrm{e}}^*} + \frac{1}{v_{\mathrm{s}}(1-\phi_{\mathrm{e}}^*)} < \frac{k_{\mathrm{spo}}k_{\mathrm{cat}}(1-e^{-\beta\Delta\mu})(D_{\mathrm{pe}}-D_{\mathrm{se}})}{v_{\mathrm{s}}(R_{\mathrm{s}}+R_{\mathrm{p}})(D_{\mathrm{pe}}R_{\mathrm{s}}+D_{\mathrm{se}}R_{\mathrm{p}})}, \quad (7)$$

where we have defined $R_{\mathrm{s}} \equiv k_{\mathrm{spo}}e^{\beta\Delta\varepsilon} + k_{\mathrm{cat}}\phi_{\mathrm{e}}^*$ and $R_{\mathrm{p}} \equiv k_{\mathrm{spo}} + k_{\mathrm{cat}}\phi_{\mathrm{e}}^* e^{-\beta(\Delta\varepsilon+\Delta\mu)}$ [30]. Since the left-hand side of Eq. (7) is always positive, an instability is possible only if the right-hand side is positive as well. The sign of the right-hand side is controlled by that of $(1-e^{-\beta\Delta\mu})(D_{\mathrm{pe}}-D_{\mathrm{se}})$, which has several implications. First, an equilibrium system with $\Delta\mu = 0$ is always stable. Second, for a catalytic reaction favoring product formation with $\Delta\mu > 0$, an instability is possible only if $D_{\mathrm{pe}} > D_{\mathrm{se}}$. Third, if $D_{\mathrm{pe}} = D_{\mathrm{se}}$ the system is always stable. Intuitively, the instability arises from opposing gradients of substrate and product generated around an enzyme-rich region when $\Delta\mu > 0$, coupled to an unequal response of the enzyme to gradients of substrate and product when $D_{\mathrm{pe}} > D_{\mathrm{se}}$, resulting in effective enzyme-enzyme attractive interactions and further aggregation. Interestingly, the instability is favored when $v_{\mathrm{e}} \gg v_{\mathrm{s}}$, which happens to correspond to the typical relative sizes of enzymes and substrates in biological systems. In Figs. 2(a) and 2(b), the unstable region delimited by Eq. (7) is shown as a function of the catalytic rate k_{cat} and the nonequilibrium drive $\Delta\mu$.

The numerical solution of the evolution equations, Eqs. (3)–(5), confirms the existence of this instability. We initialize a 1D system with small number-conserving random variations around ϕ_i^*. When the system is unstable, regions of high and low enzyme concentrations develop spontaneously [see Fig. 2(c)] and coarsen over time, ultimately resulting in two distinct phase-separated domains. Moreover, varying the amount of enzyme in the system only changes the relative size of the high and low concentration domains, without affecting the concentration values in the two domains, which suggests the existence of a binodal line, as in equilibrium phase separation. We observed this behavior for all parameters which we simulated ($k_{\mathrm{cat}}/k_{\mathrm{spo}} \approx 1-100$, $v_{\mathrm{e}}/v_{\mathrm{s}} \approx 2-100$, $-\Delta\varepsilon \approx 5-30k_BT$, $\Delta\mu \approx 5-50k_BT$, $D_{\mathrm{pe}}/D_{\mathrm{se}} \approx 1-100$). The observation of macroscopic phase separation, rather than pattern formation or microphase separation, is further supported by the linear stability analysis showing an instability at the largest wavelengths ($q^2 \to 0$), rather than at finite wavelengths. We also note that studies of two-component mass-conserving reaction-diffusion systems, which have significant parallels to the model studied here [30], have shown that these systems exhibit uninterrupted coarsening leading to macrophase separation at long times [31,32].

Effective free energy and binodal.—In the macroscopic limit, we expect the substrate-product equilibrium in the bulk of each phase to be governed by the reaction terms that act locally, rather than by spatial diffusion. This implies that the substrate and product concentrations are enslaved to the enzyme concentration by $\phi_{\mathrm{s}} \approx \phi_{\mathrm{s}}^*(\phi_{\mathrm{e}})$ and $\phi_{\mathrm{p}} \approx \phi_{\mathrm{p}}^*(\phi_{\mathrm{e}})$, with the functions defined in Eq. (6). Substituting these expressions into Eq. (3), we can recast the dynamics of the enzyme as $\dot{\phi}_{\mathrm{e}} \approx \nabla \cdot (M_{\mathrm{ee}}\nabla\mu_{\mathrm{eff}})$ with an effective chemical potential for the enzyme

$$\frac{\mu_{\mathrm{eff}}(\phi_{\mathrm{e}})}{k_BT} = \log\phi_{\mathrm{e}} - \frac{v_{\mathrm{e}}}{v_{\mathrm{s}}}\log[D_{\mathrm{se}}\phi_{\mathrm{s}}^*(\phi_{\mathrm{e}}) + D_{\mathrm{pe}}\phi_{\mathrm{p}}^*(\phi_{\mathrm{e}})]. \quad (8)$$

We can also identify an effective free energy density $f_{\mathrm{eff}}(\phi_{\mathrm{e}})$, such that $\mu_{\mathrm{eff}} = v_{\mathrm{e}}(df_{\mathrm{eff}}/d\phi_{\mathrm{e}})$, which can be explicitly calculated by direct integration [30]. By employing the common-tangent construction in unstable cases, we can identify two coexisting phases and define the binodal lines, which show good agreement with our numerical results and meet the spinodal line at a critical point; see Figs. 2(a) and 2(b).

The role of solvent.—While we have so far considered an enzyme-substrate-product system for simplicity, we observe that an instability can also occur in the presence of an additional solvent, typically water, in which these components will be dissolved. We can add a fourth component of volume fraction ϕ_{w} to the dynamics and

study the stability of the homogeneous steady state [30]. We find that the uniform steady state can be unstable even when all the solute components (enzyme, substrate, and product) are in dilute conditions, as shown in Fig. 2(d). This demonstrates the wide reach of this Letter and its potential application to realistic systems. For the remainder of this Letter, however, we focus on the simpler $\phi_w = 0$ case.

Enzymatic autoregulation.—A biologically pertinent question is what happens to the enzymatic activity when the system phase separates. The average rate of catalysis in a region of size L is given by $\bar{r}_{cat} = (1/L)\int_0^L r_{cat} dx$ in a simple 1D case. In a homogeneous state, r_{cat} will be constant throughout the system and, using Eq. (2), will go as $\bar{r}_{cat}^{(h)} \sim \phi_e(1-\phi_e)$ which is a concave function of ϕ_e. In a phase-separated state, $\bar{r}_{cat}$ is a weighted average of the catalytic rates in each phase, with the weights determined by the lever rule. From the concavity of $\bar{r}_{cat}^{(h)}$, we find that the catalytic rate in the phase-separated state is always smaller than in the homogeneous state; see Fig. 3(a). We observe a similar behavior when we vary a control parameter such as $\Delta\mu$, which is controlled by the concentration of the fuel molecules in an experiment; see Fig. 3(b). In the homogeneous phase, $\bar{r}_{cat}$ initially rises and then saturates with increasing $\Delta\mu$. The phase separation reduces $\bar{r}_{cat}$ in the whole system and leads to saturation at a lower activity. Through this mechanism, CIPS can act to autoregulate the enzymatic activity of the mixture: once the activity reaches a threshold, the system phase separates and gives rise to a reduced overall catalytic rate. A similar saturation effect is seen when other system parameters, such as k_{cat}, are varied causing the system to phase separate.

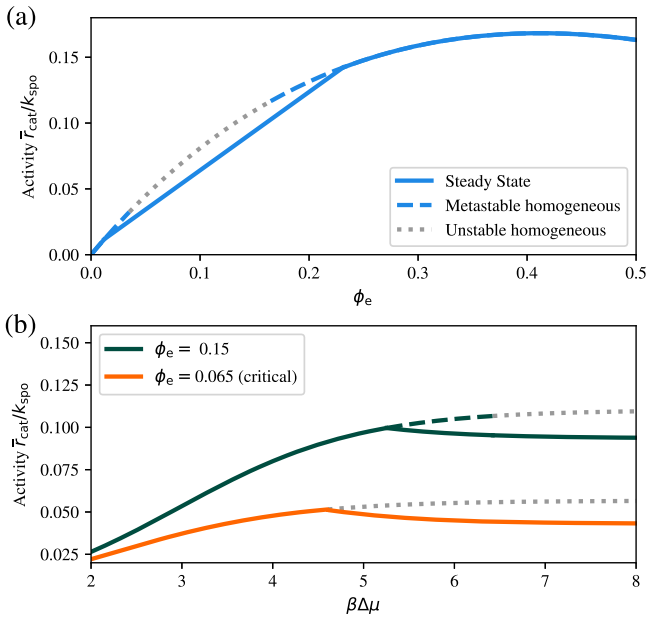

FIG. 3. Effect of CIPS on catalytic activity. (a) Activity as a function of the initial ϕ_e. In the phase-separated state, the activity is a linear combination of the activity of the homogeneous states on either side of the binodal, which due to convexity is always smaller than that of the homogeneous state. (b) Evolution of activity with increasing $\Delta\mu$. As the system phase separates, the overall catalytic rate is reduced. When $\phi_e = 0.065$, the system passes through the critical point, and there is no metastable homogeneous branch. System parameters are as in Fig. 2.

Discussion.—Using a thermodynamically consistent description of a multicomponent fluid based on linear response theory constructed from a Flory-Huggins free energy, we have identified a new, purely nonequilibrium mechanism for phase separation as a consequence of the catalytic, fueled conversion between two components (substrate and product) by a third component (enzyme). Besides the catalytic activity, a necessary ingredient for CIPS is an asymmetry in the off diagonal response coefficients (mobilities) that couple enzyme-substrate and enzyme-product thermodynamic forces and fluxes in the nonequilibrium conserved dynamics. Using a mapping of the three-component system to a single-component system with an effective free energy, equilibriumlike features of CIPS such as binodal lines were obtained.

We argue that the substrate-vs-product mobility asymmetry required for CIPS to operate can plausibly exist in realistic systems. For a typical biological catalytic process, we expect both the spontaneous and catalyzed reactions to be strongly driven, and the enzyme protein to be much larger than the small molecular substrate and product. In this biologically realistic limit, we find [30] that CIPS occurs at low enzyme concentrations whenever $(D_{pe} - D_{se})/D_{se} > k_{spo}/k_{cat}$. Given that the kinetics of catalyzed reactions are generally much faster than those of spontaneous ones (reduced energy barrier, with $k_{cat} \gg k_{spo}$), this implies that the threshold mobility asymmetry required for CIPS can become vanishingly small. While measurements of the off diagonal Onsager mobilities for biologically relevant enzyme-substrate-product systems do not exist at present to the best of our knowledge, measurements of the functionally equivalent (see the Supplemental Material [30]) Maxwell-Stefan diffusivities of various multicomponent mixtures suggest that even small changes in molecular structure (e.g., shape, polarity, etc.) of the mixture components can result in substantial changes to the mobilities [33–37].

The mechanism behind CIPS is reminiscent of mechanisms for chemotactic or phoretic aggregation previously described in the literature in the context of interacting microorganisms or catalytically active colloids [21–23,25]. However, these studies were based on microscopic descriptions of the chemotactic or phoretic response, typically valid only under dilute conditions. We expect that such microscopic descriptions and the thermodynamic-phenomenological description presented here are two sides of the same coin, the former being applicable arbitrarily far from equilibrium in dilute conditions, the latter near equilibrium at arbitrary densities. Indeed, a connection can be formally

established between the off diagonal Onsager mobilities and phoretic mobilities [22,38] or, equivalently, the Fickian cross-diffusion coefficients [37] (see the Supplemental Material [30] for details). The existing experimental observations [39,40] of the unequal response of enzymes to gradients of substrate and product thus further corroborate the assertion that an asymmetry may generically exist between the enzyme-substrate and enzyme-product Onsager mobilities.

When the enzymatic activity in the homogeneous system is increased beyond a critical threshold, for example via external factors such as the availability of fuel molecules, the system phase separates, causing the overall enzymatic activity of the system to suddenly decrease and then plateau. In multistep metabolic pathways, the production of intermediate metabolites is known to regulate other reactions in the networks and thus act as a feedback mechanism that inhibits overall metabolic activity [41,42]. CIPS provides a novel mechanism for this complex control of metabolism which, somewhat uniquely, autoregulates a single-step catalytic reaction and provides a simpler mechanism, potentially more amenable to fine-tuned synthetic control. It remains to be seen how CIPS affects catalytic activity in multistep metabolic reactions involving several distinct enzymes. We speculate that, in a system with several enzyme components, CIPS may allow for colocalization of distinct enzymes within the same aggregate, allowing for substrate channeling as in cellular metabolons [16,18]. Indeed, we previously showed that this behavior is possible in mixtures of phoretic active colloids [23].

Owing to its nonequilibrium nature, CIPS results in phase-separated states with nonvanishing fluxes, and is distinct from equilibrium mechanisms for phase separation. The latter rely on the presence of interaction terms (e.g., $\chi_{ij}\phi_i\phi_j$ and $\kappa_{ij}\nabla\phi_i\cdot\nabla\phi_j$) in the free energy density f_{FH}, which may be of enthalpic (temperature-independent) or entropic (temperature-dependent) origin. In particular, despite also requiring a size difference between components, CIPS is distinct from the entropic phase separation induced by depletion effects that is observed in binary hard-core mixtures [43], which results in equilibrium phase-separated states with vanishing fluxes. Future work may explore the competition or cooperation between equilibrium interactions and nonequilibrium catalytic effective interactions in phase separation. In particular, we note that we have focused here on effective interactions that are attractive, i.e., those with $(1-e^{-\beta\Delta\mu})(D_{\mathrm{pe}}-D_{\mathrm{se}})>0$ so that the right-hand side of Eq. (7) is positive. One may also consider repulsive effective interactions, with $(1-e^{-\beta\Delta\mu})(D_{\mathrm{pe}}-D_{\mathrm{se}})<0$. In this case, we expect that an enzyme-rich condensate held together by equilibrium interactions may be *dissolved* by sufficiently strong nonequilibrium catalytic activity. This further highlights how the mechanism we have uncovered goes well beyond the prototypical example presented here, and may prove an important player in the description of phase separation in out-of-equilibrium systems.

This work has received support from the Max Planck School Matter to Life and the MaxSynBio Consortium, which are jointly funded by the Federal Ministry of Education and Research (BMBF) of Germany, and the Max Planck Society. M. C. was supported by funding from the Biotechnology and Biological Sciences Research Council (UKRI-BBSRC) [Grant No. BB/T008784/1].

*ramin.golestanian@ds.mpg.de
†jaime.agudo@ds.mpg.de

[1] S. F. Banani, H. O. Lee, A. A. Hyman, and M. K. Rosen, Biomolecular condensates: Organizers of cellular biochemistry, Nat. Rev. Mol. Cell Biol. **18**, 285 (2017).
[2] Y. Shin and C. P. Brangwynne, Liquid phase condensation in cell physiology and disease, Science **357**, eaaf4382 (2017).
[3] C. P. Brangwynne, P. Tompa, and R. V. Pappu, Polymer physics of intracellular phase transitions, Nat. Phys. **11**, 899 (2015).
[4] J. Berry, C. P. Brangwynne, and M. Haataja, Physical principles of intracellular organization via active and passive phase transitions, Rep. Prog. Phys. **81**, 046601 (2018).
[5] S. Mao, D. Kuldinow, M. P. Haataja, and A. Košmrlj, Phase behavior and morphology of multicomponent liquid mixtures, Soft Matter **15**, 1297 (2019).
[6] S. Mao, M. S. Chakraverti-Wuerthwein, H. Gaudio, and A. Košmrlj, Designing the Morphology of Separated Phases in Multicomponent Liquid Mixtures, Phys. Rev. Lett. **125**, 218003 (2020).
[7] W. M. Jacobs, Self-Assembly of Biomolecular Condensates with Shared Components, Phys. Rev. Lett. **126**, 258101 (2021).
[8] K. Shrinivas and M. P. Brenner, Phase separation in fluids with many interacting components, Proc. Natl. Acad. Sci. U.S.A. **118**, e2108551118 (2021).
[9] C. A. Weber, D. Zwicker, F. Jülicher, and C. F. Lee, Physics of active emulsions, Rep. Prog. Phys. **82**, 064601 (2019).
[10] J. Kirschbaum and D. Zwicker, Controlling biomolecular condensates via chemical reactions, J. R. Soc. Interface **18**, 20210255 (2021).
[11] Y. I. Li and M. E. Cates, Non-equilibrium phase separation with reactions: A canonical model and its behaviour, J. Stat. Mech. (2020) 053206.
[12] R. Wittkowski, A. Tiribocchi, J. Stenhammar, R. J. Allen, D. Marenduzzo, and M. E. Cates, Scalar φ^4 field theory for active-particle phase separation, Nat. Commun. **5**, 4351 (2014).
[13] E. Tjhung, C. Nardini, and M. E. Cates, Cluster Phases and Bubbly Phase Separation in Active Fluids: Reversal of the Ostwald Process, Phys. Rev. X **8**, 031080 (2018).
[14] S. Saha, J. Agudo-Canalejo, and R. Golestanian, Scalar Active Mixtures: The Nonreciprocal Cahn-Hilliard Model, Phys. Rev. X **10**, 041009 (2020).

[15] Z. You, A. Baskaran, and M. C. Marchetti, Nonreciprocity as a generic route to traveling states, Proc. Natl. Acad. Sci. U.S.A. **117**, 19767 (2020).
[16] L. J. Sweetlove and A. R. Fernie, The role of dynamic enzyme assemblies and substrate channelling in metabolic regulation, Nat. Commun. **9**, 2136 (2018).
[17] A. Testa, M. Dindo, A. A. Rebane, B. Nasouri, R. W. Style, R. Golestanian, E. R. Dufresne, and P. Laurino, Sustained enzymatic activity and flow in crowded protein droplets, Nat. Commun. **12**, 6293 (2021).
[18] L. Poshyvailo, E. von Lieres, and S. Kondrat, Does metabolite channeling accelerate enzyme-catalyzed cascade reactions?, PLoS One **12**, e0172673 (2017).
[19] J. Agudo-Canalejo, T. Adeleke-Larodo, P. Illien, and R. Golestanian, Synchronization and Enhanced Catalysis of Mechanically Coupled Enzymes, Phys. Rev. Lett. **127**, 208103 (2021).
[20] B. Niebel, S. Leupold, and M. Heinemann, An upper limit on Gibbs energy dissipation governs cellular metabolism, Nat. Metab. **1**, 125 (2019).
[21] S. Saha, R. Golestanian, and S. Ramaswamy, Clusters, asters, and collective oscillations in chemotactic colloids, Phys. Rev. E **89**, 062316 (2014).
[22] R. Golestanian, Phoretic active matter, arXiv:1909.03747.
[23] J. Agudo-Canalejo and R. Golestanian, Active Phase Separation in Mixtures of Chemically Interacting Particles, Phys. Rev. Lett. **123**, 018101 (2019).
[24] B. Nasouri and R. Golestanian, Exact Phoretic Interaction of Two Chemically Active Particles, Phys. Rev. Lett. **124**, 168003 (2020).
[25] E. F. Keller and L. A. Segel, Initiation of slime mold aggregation viewed as an instability, J. Theor. Biol. **26**, 399 (1970).
[26] S. R. de Groot and P. Mazur, *Non-Equilibrium Thermodynamics* (Dover Publications, New York, 1984).
[27] K. W. Kehr, K. Binder, and S. M. Reulein, Mobility, interdiffusion, and tracer diffusion in lattice-gas models of two-component alloys, Phys. Rev. B **39**, 4891 (1989).
[28] E. J. Kramer, P. Green, and C. J. Palmstrøm, Interdiffusion and marker movements in concentrated polymer-polymer diffusion couples, Polymer **25**, 473 (1984).
[29] S. Bo, L. Hubatsch, J. Bauermann, C. A. Weber, and F. Jülicher, Stochastic dynamics of single molecules across phase boundaries, Phys. Rev. Research **3**, 043150 (2021).
[30] See Supplemental Material at http://link.aps.org/supplemental/10.1103/PhysRevLett.129.158101 for details on the calculation of the instability condition in the absence and presence of solvent; the explicit expression for the effective free energy and binodals; and the connections of our formalism to reaction-diffusion systems, cross-diffusion and phoretic systems, and Maxwell-Stefan diffusion.
[31] F. Brauns, J. Halatek, and E. Frey, Phase-Space Geometry of Mass-Conserving Reaction-Diffusion Dynamics, Phys. Rev. X **10**, 041036 (2020).
[32] F. Brauns, H. Weyer, J. Halatek, J. Yoon, and E. Frey, Wavelength Selection by Interrupted Coarsening in Reaction-Diffusion Systems, Phys. Rev. Lett. **126**, 104101 (2021).
[33] R. Taylor and R. Krishna, *Multicomponent Mass Transfer* (John Wiley & Sons, New York, 1993).
[34] G. Guevara-Carrion, T. Janzen, Y. M. Muñoz-Muñoz, and J. Vrabec, Mutual diffusion of binary liquid mixtures containing methanol, ethanol, acetone, benzene, cyclohexane, toluene, and carbon tetrachloride, J. Chem. Phys. **144**, 124501 (2016).
[35] G. Guevara-Carrion, Y. Gaponenko, A. Mialdun, T. Janzen, V. Shevtsova, and J. Vrabec, Interplay of structure and diffusion in ternary liquid mixtures of benzene + acetone + varying alcohols, J. Chem. Phys. **149**, 064504 (2018).
[36] B. Ramm, A. Goychuk, A. Khmelinskaia, P. Blumhardt, H. Eto, K. A. Ganzinger, E. Frey, and P. Schwille, A diffusiophoretic mechanism for ATP-driven transport without motor proteins, Nat. Phys. **17**, 850 (2021).
[37] V. K. Vanag and I. R. Epstein, Cross-diffusion and pattern formation in reaction–diffusion systems, Phys. Chem. Chem. Phys. **11**, 897 (2009).
[38] J. L. Anderson, Colloid transport by interfacial forces, Annu. Rev. Fluid Mech. **21**, 61 (1989).
[39] J. Agudo-Canalejo, T. Adeleke-Larodo, P. Illien, and R. Golestanian, Enhanced diffusion and chemotaxis at the nanoscale, Acc. Chem. Res. **51**, 2365 (2018).
[40] Y. Zhang and H. Hess, Chemically-powered swimming and diffusion in the microscopic world, Nat. Rev. Chem. **5**, 500 (2021).
[41] J. D. OConnell, A. Zhao, A. D. Ellington, and E. M. Marcotte, Dynamic reorganization of metabolic enzymes into intracellular bodies, Annu. Rev. Cell Dev. Biol. **28**, 89 (2012).
[42] M. T. Alam, V. Olin-Sandoval, A. Stincone, M. A. Keller, A. Zelezniak, B. F. Luisi, and M. Ralser, The self-inhibitory nature of metabolic networks and its alleviation through compartmentalization, Nat. Commun. **8**, 16018 (2017).
[43] D. Frenkel and A. A. Louis, Phase Separation in Binary Hard-Core Mixtures: An Exact Result, Phys. Rev. Lett. **68**, 3363 (1992).